



A LETTERS JOURNAL EXPLORING
THE FRONTIERS OF PHYSICS

OFFPRINT

**Investigation of near-field optical tweezers
based on the edge effect of extraordinary
optical transmission in thin microcavity**

LIN ZHANG and JIU HUI WU

EPL, 143 (2023) 15001

Please visit the website
www.epljournal.org

Note that the author(s) has the following rights:

- immediately after publication, to use all or part of the article without revision or modification, **including the EPLA-formatted version**, for personal compilations and use only;
- no sooner than 12 months from the date of first publication, to include the accepted manuscript (all or part), **but not the EPLA-formatted version**, on institute repositories or third-party websites provided a link to the online EPL abstract or EPL homepage is included.

For complete copyright details see: <https://authors.epljournal.net/documents/copyright.pdf>.



epl

A LETTERS JOURNAL EXPLORING
THE FRONTIERS OF PHYSICS

AN INVITATION TO SUBMIT YOUR WORK

epljournal.org

The Editorial Board invites you to submit your Letters to EPL

Choose EPL, and you'll be published alongside original, innovative Letters in all areas of physics. The broad scope of the journal means your work will be read by researchers in a variety of fields; from condensed matter, to statistical physics, plasma and fusion sciences, astrophysics, and more.

Not only that, but your work will be accessible immediately in over 3,300 institutions worldwide. And thanks to EPL's green open access policy you can make it available to everyone on your institutional repository after just 12 months.

Run by active scientists, for scientists

Your work will be read by a member of our active and international Editorial Board, led by Bart Van Tiggelen. Plus, any profits made by EPL go back into the societies that own it, meaning your work will support outreach, education, and innovation in physics worldwide.



epljournal.org

In 2020

Manuscripts published
received

150

downloads on average

In 2020

Perspective papers received

350

downloads on average

In 2020

“Editor’s Choice”
articles received

500

downloads on average

*We greatly appreciate
the efficient, professional
and rapid processing of our
paper by your team.*

Cong Lin
Shanghai University

Four good reasons to publish with EPL

- 1 International reach** – more than 3,300 institutions have access to EPL globally, enabling your work to be read by your peers in more than 90 countries.
- 2 Exceptional peer review** – your paper will be handled by one of the 60+ co-editors, who are experts in their fields. They oversee the entire peer-review process, from selection of the referees to making all final acceptance decisions.
- 3 Fast publication** – you will receive a quick and efficient service; the median time from submission to acceptance is 78 days, with an additional 28 days from acceptance to online publication.
- 4 Green and gold open access** – your Letter in EPL will be published on a green open access basis. If you are required to publish using gold open access, we also offer this service for a one-off author payment. The Article Processing Charge (APC) is currently €1,480.

Details on preparing, submitting and tracking the progress of your manuscript from submission to acceptance are available on the EPL submission website, epletters.net.

If you would like further information about our author service or EPL in general, please visit epljournal.org or e-mail us at info@epljournal.org.

EPL is published in partnership with:



European Physical Society



Società Italiana di Fisica

edp sciences **IOP Publishing**

EDP Sciences

IOP Publishing

Investigation of near-field optical tweezers based on the edge effect of extraordinary optical transmission in thin microcavity

LIN ZHANG^(a) and JIU HUI WU^(b)

*School of Mechanical Engineering, Xi'an Jiaotong University - Xi'an 710049, China and
State Key Laboratory for Strength and Vibration of Mechanical Structures, Xi'an Jiaotong University
Xi'an 710049, China*

received 6 May 2023; accepted in final form 22 June 2023

published online 4 July 2023

Abstract – Optical tweezers are powerful tools capable to trap and manipulate particles directly. However, using conventional optical tweezers for nanosized objects remains a formidable challenge due to the optical diffraction limits and high-power levels required for nanoscale trapping, which usually causes irreversible damage to the captured particles. In this paper, we investigate the near-field edge effect of thin microcavity due to macroscopic quantum effect, and the highly enhanced electric field can reach 2.4 times. Thus, a dual near-field optical trap potential well is generated at the edge of the thin microcavity. We theoretically show that this near-field potential well can stably capture nanoparticles smaller than 10 nm while keeping the incident optical power level below 100 mW. Besides, the relationship between size of the microcavity and optical gradient force has also been carefully studied. Finally, the theoretical model of near-field optical tweezers with double thin microcavity is established, and the electric field magnitude of the double microcavity model is enhanced by 4.5 times compared with single microcavity model, in which the coupling effect of double hole makes smaller particles be stably trapped. Our research presents a huge potential for optical trapping and separation of nanoparticles and biomolecules.

Copyright © 2023 EPLA

Introduction. – Since Ashkin captured and manipulated a micronized glass sphere using a microscopic objective after focusing a laser beam in 1986 [1–3], optical tweezers have been widely used and developed due to their noncontact nature and inherent high precision over the next 30 years [4,5]. Their principle is that dielectric particles can both accelerate in the direction of the beam and get trapped in regions of high optical intensity upon interaction with light. Therefore, optical tweezers overcome the defects of traditional mechanical operation and become a powerful means of probing and controlling micrometer-scale objects. For example, in the biosciences, optical tweezers have been widely utilized to trap a single living cell or protein [6], bacteria [7], virus particles [8], and DNA molecule [9]. In physics, optical tweezers have enabled the cooling and trapping of neutral atoms [10], the fabrication of atomic clocks, and the accurate measurement of forces [11].

Despite the immense application potential of optical tweezers in numerous subject areas, capturing and classifying particles whose size is much smaller than the

wavelength of light remains a significant challenge for optical tweezers. There are two reasons to hamper the accuracy of optical tweezers. First, affected by the diffraction limit of light, the physical size of the potential well generated by optical tweezers is much larger than that of nanoscale particles, which leads to the imprecise trapping.

Second, when the particle size is much smaller than the wavelength, according to the Rayleigh model, the optical gradient force of the dielectric particle is proportional to the third power of the particle radius d^3 [12]. Therefore, as the size decreases, the particle trapping increases dramatically. To overcome this problem, increasing the light intensity is required, which will cause damage to the sample.

In recent years, near-field optical tweezers have been developed greatly, the evanescent field generated not only breaks through the diffraction limit, but also decays exponentially in the direction away from the interface [13–15]. These two properties effectively reduce the size of the optical potential well and also increase the optical tweezers forces due to the enhanced field intensity gradient. Now near-field optical tweezers based on aperture probes, photonic crystal (PC) cavities and nanofibers have developed the optical manipulation for smaller sizes,

^(a)E-mail: zhlforever@stu.xjtu.edu.cn

^(b)E-mail: ejhwu@mail.xjtu.edu.cn (corresponding author)

higher efficiency and larger quantities. For instance, localized surface plasmons are excited to trap nanoparticles in a liquid environment by illuminating the tip of the metal probe with a laser [16]. Besides, photonic crystal cavities reduce the power threshold for stable trapping due to the significant increase of optical field strength [17]. Meanwhile, a pair of nano waveguide coupling arrays is capable to trap and separate nanoparticles ranging in size from 100 to 200 nm [18].

In this paper, we propose using thin microcavity as optical trap. According to the existing results, a near-field optical diffraction model for a thin microcavity embedded within a thin conducting film was presented, using which all electromagnetic field components both inside and outside the microcavity were derived accurately, and the near-field edge effect was comprehended by numerical computations [19,20]. We investigate the edge effect of thin microcavity due to macroscopic quantum effect, and the highly enhanced electric field can reach 2.4 times [21–23]. Thus, a dual near-field optical trap potential well is generated at the edge of the thin microcavity. Here, we systematically research the optical force and potential experienced by dielectric particle interacting with the near-field scattering of thin microcavity. In addition, the theoretical model of near-field optical tweezers with double thin microcavity is established [24], in which the coupling effect of double hole makes smaller particles be stably trapped. Our research indicates that this near-field potential well can stably capture nanoparticles smaller than 5 nm while keeping the incident optical power level below 100 mW.

Theory of near-field optical tweezers with thin microcavity. – Figure 1(a) shows the schematic of near-field thin microcavity optical tweezers, which consists of semiconductor laser, thin microcavity and microfluidic chamber containing nanoparticles. As the trapping laser, we choose incident light with power of 100 nW to irradiate vertically in the thin microcavity, and its expression is $\Phi_i = E_0 \exp(ik_0 z) \mathbf{y}$. The microfluidic chamber is sealed on the lower surface of the thin microcavity by glass, and nanoparticles are suspended in water so that the small contribution from gravity pulls the nanoparticles away from the thin microcavity. In addition, the optical force acts against the particle's gravity and Brownian force.

Figure 1(b) shows the sketch of thin microcavity, which is a silver ring with aperture r and thickness h . Based on our earlier theory of the near-field thin microcavity, the electric and magnetic field components along x , y , and z directions are labeled as E_1 , E_2 , E_3 and H_1 , H_2 , H_3 . By applying the power flow theorem and the variable theorem, the following equation for the time-harmonic magnetic field of thin microcavity can be obtained:

$$\nabla^4 H_3 - k^4 H_3 = \frac{-3i\omega\epsilon}{h^2} \left[\frac{\partial E_{3U}}{\partial z} \Big|_{z=\frac{h}{2}} - \frac{\partial E_{3D}}{\partial z} \Big|_{z=-\frac{h}{2}} \right], \quad (1)$$

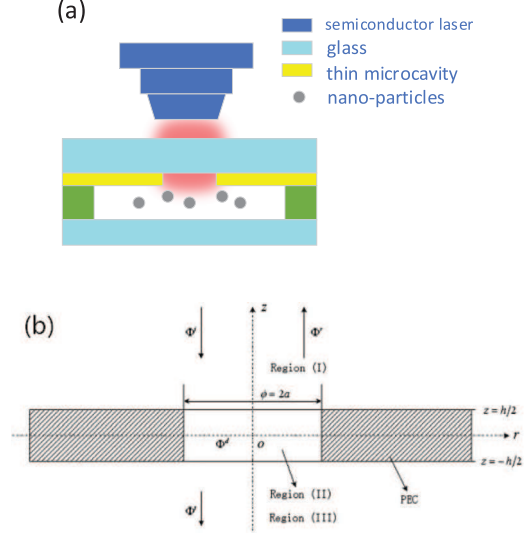


Fig. 1: (a) Schematic drawing of the near-field thin microcavity optical tweezers, (b) geometric sketch of thin microcavity.

where $\nabla^4 = \partial^4/\partial x^4 + 2\partial^4/\partial x^2\partial y^2 + \partial^4/\partial y^4$, k is the propagation constant in thin microcavity ($k^4 = (\mu\epsilon\omega^2 h^2 - 36)\mu\epsilon\omega^2/h^2$), ϵ is the permittivity of the thin microcavity. E_{3U} and E_{3D} are the electric field components in the z -direction on the upper and lower surfaces of the thin microcavity.

The magnetic field component H_3 in thin microcavity can be obtained as

$$H_3 = \sum_{n=0}^{\infty} \left[A_n J_n(kr) + C_n I_n(kr) + E_0 r^n \frac{3}{\pi h^2 i} \frac{k_0^2}{\omega \mu k^4} e^{ik_0 h/2} \frac{(-1)^{n+1} - 1}{(n+1)n!2^{n+1}} \right] \exp(in\theta), \quad (2)$$

where $A_n J_n(kr)$ and $C_n I_n(kr)$ are the general solutions of equation, n represents the different modes of magnetic field distribution, and (r, θ) represents the coordinates of different positions in the thin microcavity.

In addition, the reflected Φ_r and transmitted field components Φ_t in the upper (Region I) and lower (Region III) spaces can be expressed in polar coordinates using the linear superposition method as follows:

$$\Phi_r(r, \theta, z) = \sum_{n=-\infty}^{\infty} \int_0^{\infty} \tilde{\Phi}_r(\rho) J_n(\rho r) e^{i\sqrt{k_0^2 - \rho^2}(z-h/2)} \rho d\rho e^{in\theta}, \quad (3)$$

$$\Phi_t(r, \theta, z) = \sum_{n=-\infty}^{\infty} \int_0^{\infty} \tilde{\Phi}_t(\rho) J_n(\rho r) e^{-i\sqrt{k_0^2 - \rho^2}(z+h/2)} \rho d\rho e^{in\theta}, \quad (4)$$

where J_n is the Bessel function of first kind, $\tilde{\Phi}_r(\rho)$ is the Hankel transform of $\Phi_r(r, 0, h/2)$, which is defined as $\int_0^{\infty} \Phi_r(r, 0, h/2) J_n(\rho r) r dr$, besides, $\tilde{\Phi}_t(\rho)$ is

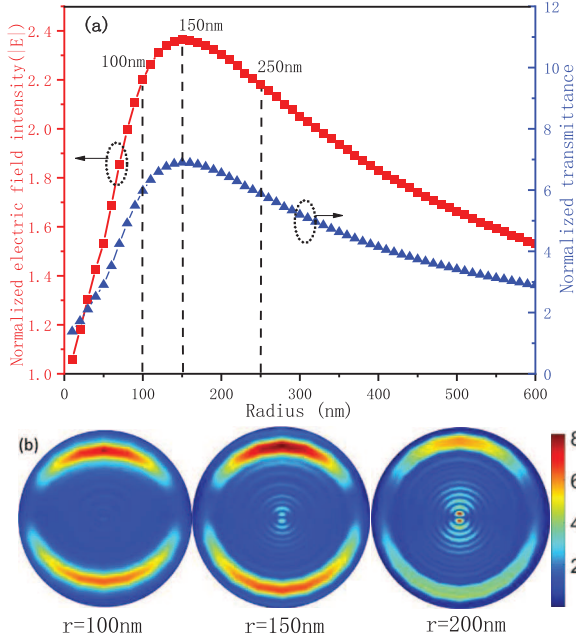


Fig. 2: (a) The transmission and normalized electric field intensity through a single thin microcavity with different radii in a range of 10–600 nm, (b) the electric field distribution at the radius of 100, 150, and 250 nm.

the Hankel transform of $\Phi_t(r, 0, -h/2)$, which is defined as $\int_0^\infty \Phi_t(r, 0, -h/2) J_n(\rho r) r dr$, here $\Phi_r(r, 0, h/2)$ represents E_{1U} , E_{2U} , H_{1U} and H_{2U} , and $\Phi_t(r, 0, -h/2)$ represents E_{1D} , E_{2D} , H_{1D} and H_{2D} .

Based on the approach given above, the electromagnetic field distribution in microfluidic chamber under the thin microcavity can be accurately obtained. We first analyze the relationships between the transmittance and the structural parameters of thin microcavity. Figure 2(a) illustrates the normalized electric field intensity (E_{norm}) and transmittance (T_{norm}) spectrum of the aperture, and the specific calculation formula are as follows:

$$E_{norm} = \frac{\mathbf{E}_{out}}{\mathbf{E}_{in}} = \frac{\int \Phi_t ds}{\int \Phi_i ds}, \quad (5)$$

$$T_{norm} = \frac{\mathbf{P}_{out}}{\mathbf{P}_{in}} = \frac{\frac{1}{2} \int \varepsilon \Phi_t^2 ds}{\frac{1}{2} \int \varepsilon \Phi_i^2 ds}. \quad (6)$$

It is apparent from fig. 2(a) that there is an enhanced transmission peak at the radius 150 nm, where normalized electric field intensity can reach 2.4 times and the transmittance is larger than 7. This transmission peak arises from the extraordinary optical transmission (EOT) effect of thin microcavity. Figure 2(b) shows the distribution of electric field intensity of aperture 100, 150, 250 nm respectively, it can be clearly demonstrated that there is an obvious enhancement of electric field at the edge of the aperture of the thin microcavity, which is called the edge effect. When increasing the aperture size from 100 to 250 nm, the edge effect increases gradually, reaching the maximum at 150 nm of diameter, and then disappears.

Therefore, the theoretical data show a maximized edge effect close to the aperture corresponding to the EOT, which provides an opportunity for generating strong near-field optical gradient forces.

With the field distribution around the thin microcavity determined, the near-field optical gradient forces for a Rayleigh particle can be easily calculated as

$$F_{grad} = \frac{2\pi n_2 a^3}{c} \left(\frac{m^2 - 1}{m^2 + 2} \right) \nabla I(r), \quad (7)$$

where $m = n_1/n_2$, n_1 and n_2 are the refractive index of the particle and the medium, a is the radius of the particle and c is the speed of light in vacuum, $I(r)$ is the light intensity. The particle tends to move to the higher light intensity where its induced dipole has lower potential energy, the assumption inherent in eq. (7) is that the particle is too small to alter the distribution of $I(r)$. We still choose a thin microcavity parameters with $r = 150$ nm, $h = 20$ nm and the edge effect is most obvious under the light irradiation of $\lambda = 630$ nm. We study the optical traps generated on a 10 nm diameter dielectric particle interacting with this near-field in medium space ($n_2 = 1.33$), and the refractive index of the particle n_1 was set to 2. The distance between the particle and the lower surface of thin microcavity is fixed to 20 nm, and we can calculate the near-field optical gradient forces of particles at different positions.

Figure 3(a) shows the near-field optical gradient force diagram of the nanoparticle under the electric field of the thin microcavity, which includes two transverse optical force components (F_x , F_y) and one vertical optical component (F_z). Figure 3(b) shows the distribution field of transverse force in the y -direction, the corresponding fig. 3(c) shows the distribution field of transverse force in the x -direction. It can be seen from the figures above that there are positive and negative optical gradient forces, which represent different directions of force, respectively pointing to the edge effect position in the thin microcavity. When the nanoparticle is exactly at the center of the edge effect position, the total transverse forces on the nanoparticle is zero. When the nanoparticle is removed from the edge effect position due to Brownian motion, gravity, or other forces, the transverse optical gradient force will bring the nanoparticle back to the center of the hot spot. Figure 3(d) shows the distribution field of longitudinal force in the z -direction, the exponentially decaying evanescent field provided the optical gradient force of the nanoparticle, and the direction of the force was directed towards the aperture, which made the particles move towards the thin microcavity to achieve capture, as shown in fig. 3. It is worth noting that the peak value of the optical gradient force in the y -direction ($F_y^{max} = 1.06$ pN) is larger than that of the optical gradient force in the x -direction ($F_x^{max} = 0.13$ pN), and the specific relationship is satisfied by $F_y^{max} = 8F_x^{max}$. This result arises from the fact that the change of electric field gradient in the

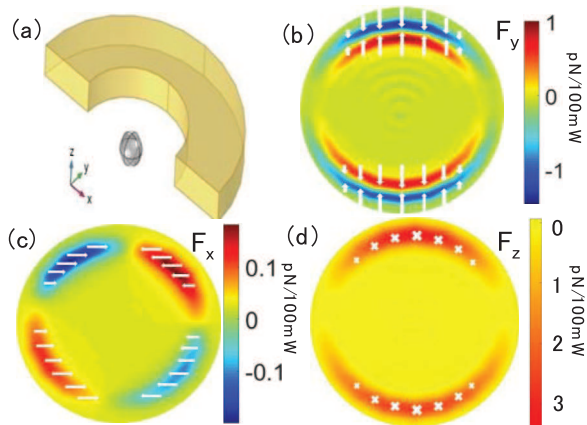


Fig. 3: (a) The near-field optical gradient force diagram of nanoparticle. (b)–(d) The transverse optical force components (F_x , F_y) and one vertical optical component (F_z) exerted on a 10-nm-diameter dielectric particle. The direction of the arrows in the diagram indicates the direction of the gradient force.

y -direction is much greater than that in the x -direction. In addition, the peak value of the optical gradient force in the z -direction $F_z^{max} = 3.2$ pN, the reason is that the electric field gradient changes exponentially in the z -direction.

The gradient force can form a trap to bind nanoparticles, which can be called the optical potential well, and the trapping potential generated by the optical force determines the stability of particle trapping. The potential well is calculated using the force fields in all directions. The potential energy in the horizontal and vertical directions at position (r_0, z_0) can be expressed as

$$U(r_0) = - \int_{\infty}^{r_0} f(r) dr, \quad (8)$$

$$U(z_0) = - \int_{\infty}^{z_0} f_z(z) dz. \quad (9)$$

In general, the nanoparticle is subjected to four forces, including gravity, buoyancy, optical gradient force and Brownian force, among which gravity and buoyancy can be ignored. The Brownian force is due to the thermal fluctuations, and a $1 k_B T$ optical potential well can be sufficient to overcome the thermal energy of the nanoparticle and locate it in an optical trap according to Einstein's wave dissipation theorem. However, nanoparticles will not escape from the potential well due to the random Brownian motion impact when the potential well depth is larger than $10 k_B T$. Figure 4(a) shows the dual optical potential well generated by the transverse forces of F_x and F_y , the data was taken using a thin microcavity with $r = 150$ nm, $h = 20$ nm to trap a 10 nm diameter dielectric particle located 15 nm away from the microcavity in the transverse plane and the incident optical power is 100 mW. The depth of the potential well is $23.1 k_B T$, and its value is greater than $10 k_B T$, thus it can stably capture nanoparticles with the diameter of 10 nm. Besides, we calculated the distribution of the optical potential well equal

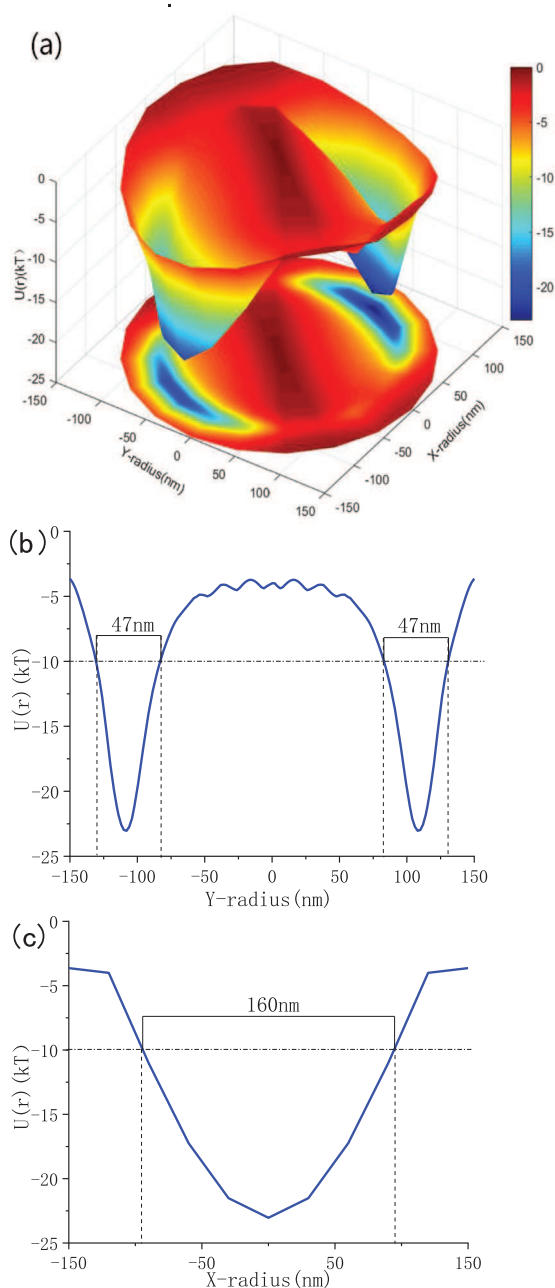


Fig. 4: (a) Transverse trapping potential generated by the transverse forces of F_x and F_y on 10 nm nanoparticle placed 20 nm away from thin microcavity. (b), (c): cross-sections of the transverse optical trapping potential ($U_r(kT)$) along $x = 0$ nm and $y = 108$ nm, where the width of stable trapping potential well ($U_r(kT) < -10 k_B T$) are indicated.

to $10 k_B T$ in the x and y directions, as shown in fig. 4(b) and (c). The width of the potential well is 47 nm in the y -direction and 160 nm in x -direction. This is because the F_y is much larger than F_x , which also indicates stronger trapping in the y -direction.

Figure 5(a) shows the effect of the distance between the nanoparticle and the thin microcavity on the vertical optical force F_z and corresponding potential well $U_z(kT)$. We

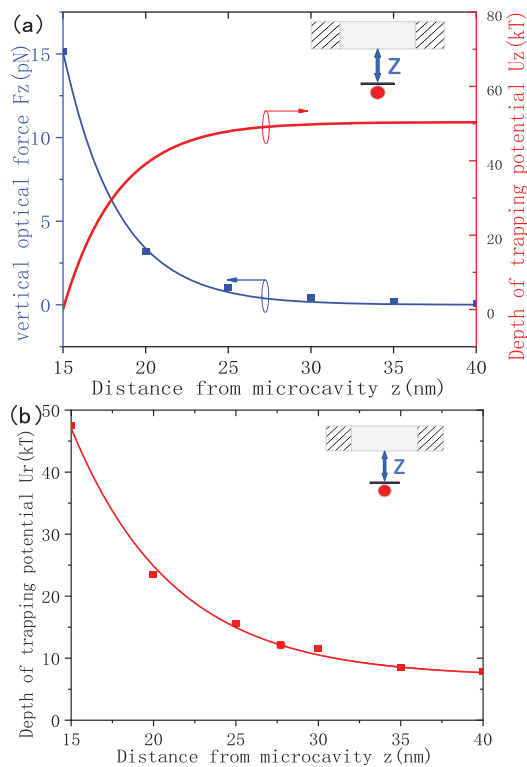


Fig. 5: (a) The effect of the distance z (nm) between the nanoparticle and the thin microcavity on the vertical optical force F_z and corresponding vertical potential well $U_z(kT)$. (b) The effect of the distance z (nm) on the transverse optical trapping potential well ($U_r(kT)$).

consider different distances (15, 20, 25, 30, 35 and 40 nm) with $r = 150$ nm, $h = 20$ nm to trap a 10 nm diameter dielectric particle, the vertical optical force F_z increases exponentially as the targeted particle approaches the thin microcavity. Therefore, the vertical trapping force pulls the particles into the thin microcavity. Figure 5(b) shows the effect of the distance between the nanoparticle and the thin microcavity on the corresponding potential well $U_r(kT)$. Similar to the F_z , the potential well $U_r(kT)$ also increases exponentially as the distance decreases.

Next, we explore the effect of the aperture of the thin microcavity on the depth of the optical trapping well with different particle sizes. We consider three different particle diameters (10, 7, and 5 nm). Figure 6 shows the depth of the optical trapping well $U_r(kT)$ at different aperture and particle sizes. Figure 6 indicates that the edge effect reaches the maximum at 150 nm of diameter, and the corresponding optical potential well is the deepest. Besides, as shown in formula (7), the optical gradient forces for the Rayleigh particle are proportional to d^3 . For instance, the depth of the optical well for three particles with different sizes at 150 nm aperture is respectively 23.1 kT, 7.93 kT, 2.91 kT, and the ratio between trapping potential of the 10 nm and the 5 nm particles is approximately 2³.

As can be seen from fig. 6 above, the thin microcavity with 150 nm aperture can trap particles as small as 10 nm

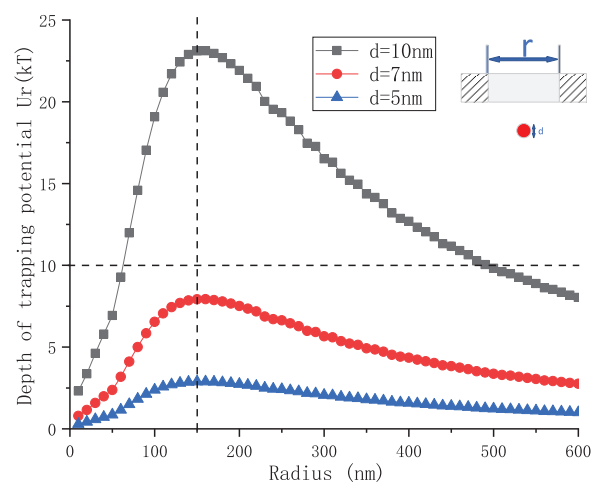


Fig. 6: The effect of the nanoparticle sizes d on the depth of trapping potential well ($U_r(kT)$).

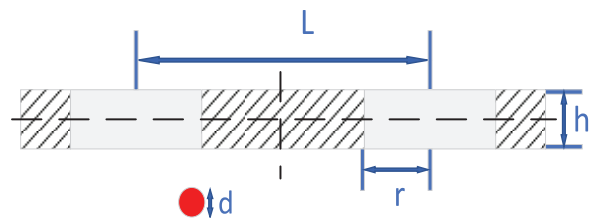


Fig. 7: The Schematic of near-field optical tweezers with double-thin microcavity.

when the incident optical power is 100 nW. However, when the particle size decreases, the trapping potential well generated by the microcavity decreases rapidly. For example, the depth of the trapping potential well for 5 nm particle is only 2.91 kT, which is far less than 10 kT. In order to improve the depth of optical potential well without increasing the incident light power, more intensity edge effect is required.

Near-field optical tweezers model with double thin microcavity. – To achieve a stronger edge effect, double-thin microcavity near-field optical tweezers were established, as shown in fig. 7. Two thin microcavities of radius r are embedded in a perfect electrically conducting thin film of thickness h and are separated by a distance L . When two thin microcavities are spaced infinitely, their electromagnetic fields inside are independent and each hole obeys the thin microcavity theory. However, when two microcavities are brought into close proximity, their electromagnetic fields are coupled with each other as a result of the interactions between their evanescent fields. Based on our previous research, the coupled field distribution of two microcavities can be obtained from the coupled mode theory.

Figure 8 shows the electric field magnitudes in y -direction from a single microcavity and double microcavity under illumination at an incident wavelength $\lambda = 630$ nm

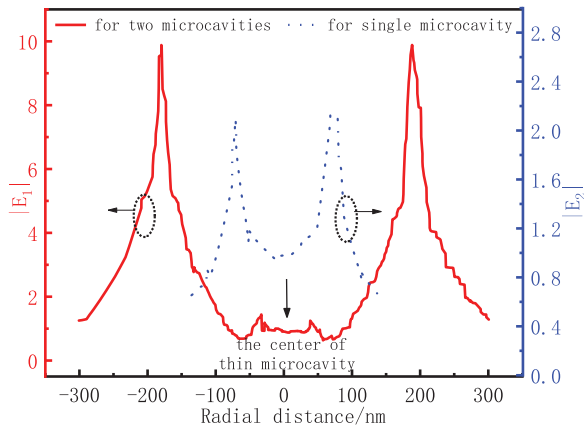


Fig. 8: The electric field magnitudes in the y -direction from a single microcavity and double microcavity under illumination at an incident wavelength $\lambda = 630$ nm in the longitudinal section where $x = 0$ at the observation point $z = -14$ nm.

in the longitudinal section where $x = 0$ at the observation point $z = -14$ nm. As shown by the red line in the figure, there is an obvious edge effect on the inner side of the two holes, which is the result of the coupling of electromagnetic fields, and the normalized electric field intensity is 10. When compared with the results for the single microcavity, the electric field magnitude of the double thin microcavity model is enhanced by 4.5 times. Therefore, the double thin microcavity model can produce a stronger effect to trap smaller nanoparticles.

Next, we investigate the effect of distance L between double thin microcavity on the edge effect. To ensure the other structural parameters remain unchanged, we set the distance L between double thin microcavity center varying from 200 to 1200 nm, besides, the electric field enhancement factor E_1/E_2 is used to describe the enhanced intensity of edge effect. The results in fig. 9 show that when L ranges from 200 to 300 nm, the enhancement factor changes slightly, the reason is that the short distance L cannot be coupled with the long wavelength. When L increases to 352 nm, there is a peak of enhancement factor at the distance $0.56(L/\lambda)$, where the enhancement factor reaches approximately 4.5 [25]. This time the evanescent wavelength propagated along the surface is matched with the double thin microcavity structure to achieve coupling. In the range of 400–1200 nm, the enhancement factor changes sinusoidally with distance L , which also satisfies the periodic coupling mode theory. In addition, the peak value of each enhancement factor decreased exponentially with increasing distance, which was due to the evanescent wave propagating along the surface of the thin microcavity which decreased exponentially.

Finally, we calculate the trapping potential well experienced by a 5 nm diameter dielectric particle ($n_1 = 2$) interacting with the near field 14 nm away from the double thin microcavity, and the superiority of the double thin microcavity structure is revealed by comparing with the single thin microcavity potential. Figure 10 shows the

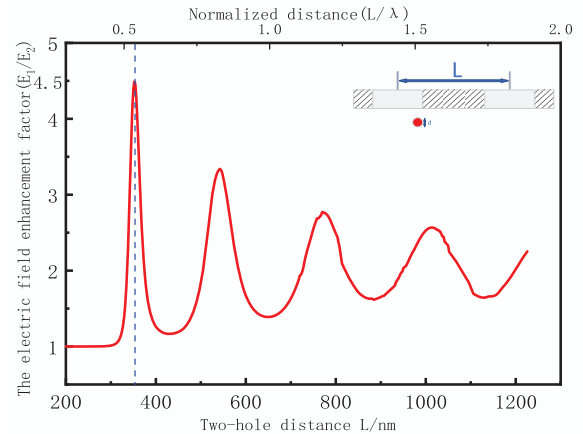


Fig. 9: The effect of two-hole distance L on the electric field enhancement factor (E_1/E_2).

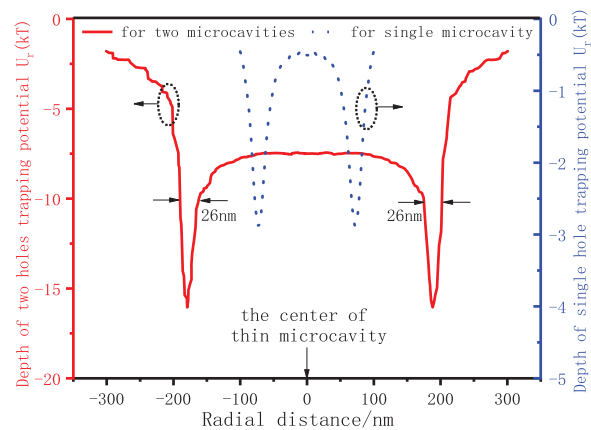


Fig. 10: Cross-sections of the transverse optical trapping potential ($U_r(kT)$) on 5 nm nanoparticle placed 14 nm away from thin microcavity along $x = 0$ nm from a single microcavity and double thin microcavity, where the width of stable trapping potential well ($U_r(kT) < -10 k_B T$) is indicated.

transverse trapping potential $U_r(kT)$ in the longitudinal section where $x = 0$ from a single microcavity and double microcavity, as shown by the red and blue lines in fig. 10.

The potential well depth generated by the single thin microcavity is $2.91 k_B T/100$ mW for trapping 5 nm particles, which is much less than $10 k_B T$. As shown by the red line in the figure, the depth of potential well by double thin microcavity increases to $16.2 k_B T/100$ mW for the same size particles. Therefore, the peak of this pulling force appears at the center of the high intensity field, which traps particles at the bottom of the potential well. Besides, the potential well width of double microcavity in the y -direction is 26 nm, which is much smaller than in single microcavity model. Thus, it can stabilize the captured particles better.

Conclusions. – In conclusion, we investigated the edge effect of thin microcavity due to macroscopic quantum effect, and the highly enhanced electric field can reach 2.4

times. Therefore, a dual near-field optical trap potential well is generated at the edge of the thin microcavity. We calculated the near-field light gradient force caused by the edge effect, which includes two transverse optical force components (F_x , F_y) and one vertical optical component (F_z), then we theoretically show that the depth of near-field potential well can reach $23.1 k_B T$ at the incident power of 100 mW when trapping 10 nm particles. Finally, the theoretical model of near-field optical tweezers with double thin microcavity is established. Due to the coupling effect of the electric field of the double thin microcavity, the electric field magnitude of the double microcavity model is enhanced by 4.5 times compared with single microcavity model, in which the coupling effect of double hole makes smaller particles be stably trapped. The above research provides theoretical support for the design and development of near-field optical tweezers.

The authors declare that they have no known competing financial interests or personal relationships that could have appeared to influence the work reported in this paper.

Data availability statement: The data that support the findings of this study are available upon reasonable request from the authors.

REFERENCES

- [1] ASHKIN A., DZIEDZIC J. M., BJORKHOLM J. E. and CHU S., *Opt. Lett.*, **11** (1986) 288.
- [2] ASHKIN A., DZIEDZIC J. M. and YAMANE T., *Nature*, **330** (1987) 769.
- [3] CHU S., BJORKHOLM J. E., ASHKIN A. and CABLE A., *Phys. Rev. Lett.*, **57** (1986) 314.
- [4] OMORI R., KOBAYASHI T. and SUZUKI A., *Opt. Lett.*, **22** (1997) 816.
- [5] OKAMOTO K. and KAWATA S., *Phys. Rev. Lett.*, **83** (1999) 4534.
- [6] BUSTAMANTE C. J., CHEMLA Y. R., LIU S. X. and WANG M. D., *Nat. Rev. Methods Primers*, **1** (2021) 25.
- [7] SHI Y. Z., ZHU T. T., ZHANG T. H., MAZZULLA A., TSAI D. P., DING W. Q., LIU A. Q., CIPPARRONE G., SAENZ J. J. and QIU C. W., *Light-Sci. Appl.*, **9** (2020) 62.
- [8] SHI Y. Z., NGUYEN K. T., CHIN L. K., LI Z. Y., XIAO L. M., CAI H., YU R. Z., HUANG W., FENG S. L., YAP P. H., LIU J. Q., ZHANG Y. and LIU A. Q., *ACS Sens.*, **6** (2021) 3445.
- [9] WANG M. D., YIN H., LANDICK R., GELLES J. and BLOCK S. M., *Biophys. J.*, **72** (1997) 1335.
- [10] YANG B., SUN H., HUANG C. J., WANG H. Y., DENG Y. J., DAI H. N., YUAN Z. S. and PAN J. W., *Science*, **369** (2020) 550.
- [11] LI H., CAO Y. Y., ZHOU L. M., XU X. H., ZHU T. T., SHI Y. Z., QIU C. W. and DING W. Q., *Adv. Opt. Photon.*, **12** (2020) 288.
- [12] KWAK E. S., ONUTA T. D., AMARIE D., POTYRAILO R., STEIN B., JACOBSON S. C., SCHAICH W. L. and DRAGNEA B., *J. Phys. Chem. B*, **108** (2004) 13607.
- [13] SALEH A. A. E. and DIONNE J. A., *Nano. Lett.*, **12** (2012) 5581.
- [14] PANG Y. J. and GORDON R., *Nano Lett.*, **11** (2011) 3763.
- [15] SHI Y. Z., SONG Q. H., TOFTUL I., ZHU T. T., YU Y. F., ZHU W. M., TSAI D. P., KIVSHAR Y. and LIU A. Q., *Appl. Phys. Rev.*, **9** (2022) 031303.
- [16] NOVOTNY L., BIAN R. X. and XIE X. S., *Phys. Rev. Lett.*, **79** (1997) 645.
- [17] JUAN M. L., GORDON R., PANG Y. J., EFTEKHARI F. and QUIDANT R., *Nat. Phys.*, **5** (2009) 915.
- [18] SHI Y. Z., XIONG S., CHIN L. K., ZHANG J. B., SER W., WU J. H., CHEN T. N., YANG Z. C., HAO Y. L., LIEBERG B., YAP P. H., TSAI D. P., QIU C. W. and LIU A. Q., *Sci. Adv.*, **4** (2018) eaao0773.
- [19] WU J. H., *Opt. Lett.*, **36** (2011) 3440.
- [20] WU J. H., LIU A. Q. and LI H. H., *Opt. Lett.*, **31** (2006) 2438.
- [21] ZHANG L. and WU J. H., *Opt. Commun.*, **475** (2020) 126256.
- [22] ZHANG L. and WU J. H., *EPL*, **138** (2022) 65001.
- [23] ZHANG L. and WU J. H., *EPL*, **142** (2023) 40002.
- [24] CHEN X., WU J. H. and CAO P., *J. Opt. (U.K.)*, **20** (2018) 105604.
- [25] RUAN Z. C. and QIU M., *Phys. Rev. Lett.*, **96** (2006) 233901.